Article

Infrared Spectrum Characteristics and Quantification of OH Groups in Coal

Fengwei Dai,* Qiuying Zhuang, Ge Huang, Hanzhong Deng, and Xun Zhang

Cite This: *ACS Omega* 2023, 8, 17064−17076

Read Online

ACCESS | Metrics & More | Article Recommendations

ABSTRACT: The KBr pellet press method for detecting the infrared spectrum of coal is one of the commonly used methods for analyzing the types and content of functional groups in coal. However, KBr crystalline water or moisture has a significant impact on the peak position, peak shape, and peak area of the organic O−H based stretching vibration wave in coal. In this paper, the theoretical characteristics of infrared spectra of phenols and alcohols have been simulated and analyzed using the Gaussian 16 series of programs. Four infrared spectral analysis techniques, in situ infrared, KBr pellet press, dry KBr pellet press, and paste methods, have been used to detect the infrared spectra of coal. The results show that the stretching vibration peaks of free O−H radicals without hydrogen bonding are located between 3700 and 3600 cm^{-1}. After the O−H form hydrogen bonds with each other, the O−H stretching vibration frequency moves toward the low frequency direction, and the lower the wavenumber, the more O−H content. The conventional KBr gasket manufacturing process will absorb moisture in the air to interfere with the hydroxyl absorption peak of coal, and the experimental process requires absolute drying. The relative content of hydroxyl in coal can be compared and analyzed based on the peak position, peak shape, and peak area of the hydroxyl stretching vibration wave. Quantitative analysis of hydroxyl groups in coal also requires combination of elemental analysis and X-ray photoelectron spectroscopy.
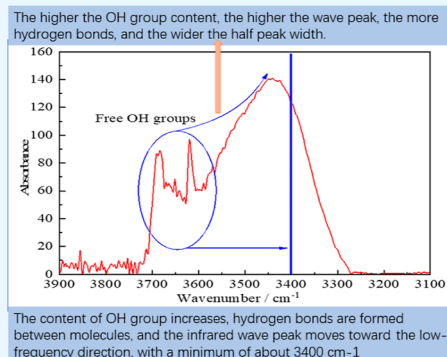
1. INTRODUCTION

With the in-depth study of the mechanism of coal spontaneous combustion, researchers have found that hydroxyl groups are an important factor leading to spontaneous combustion of coal. Therefore, the analysis and quantification of OH groups in coals are of great significance to determine the tendency of coal spontaneous combustion.

A large number of scholars have analyzed the OH groups' characteristics of coal by infrared spectroscopy. As early as 1981, Painter et al.[1,2] used this method to study the functional groups of coal. The experimental results show that there is a broadened absorption peak near 3400 cm^{-1}, belonging to OH groups and water in coal. The hydrogen bonding between the OH groups makes the infrared absorption peak wider and stronger and moves toward the direction of low wavenumber to form this peak. At the early stage, scholars[3–8] mainly studied the broadened absorption peak of O−H between 3500 and 3200 cm^{-1} of coal and discussed the type of hydrogen bond forming this peak in detail. With the deepening of research, the experimental results of Solomon et al.[4,6,7,9–17] show that the infrared spectrum of OH groups of most coal samples has a broadened absorption peak between 3500 and 3200 cm^{-1}, and some sharp small absorption peaks will appear in the area of 3700−3590 cm^{-1}. Among them, some scholars have analyzed these small sharp peaks. Solomon et al.[9,12] pointed out that the small absorption peak near 3640−3610 cm^{-1} in the infrared

spectrum of coal is the absorption peak of kaolinite. Miura et al.[4,6,7,11,18] believed that the small absorption peak of 3640−3610 cm^{-1} was free OH groups.

Xin et al.[19] have detected the infrared spectra of 15 kinds of coal samples. The results showed that O−H stretching vibration peaks of 11 kinds of high-rank coal samples appeared in the 3600−3640 cm^{-1} band and had no absorption peak in the 3400 cm^{-1} band. The O−H stretching vibration peaks of other four low-rank coal are located at 3400 cm^{-1}. The infrared spectra of five coal samples studied by Choi et al.[20] showed that there is basically no O−H peak with only small fluctuations occurring at the area of 3700−3590 cm^{-1}.

Solomon, Okolo, et al.[21,22] dried the KBr tablet of coal at different temperatures and times. The experimental results show that the broadened absorption peak near 3400 cm^{-1} decreases, while the absorption peak such as the stretching vibration of CH bond does not change, indicating that KBr−
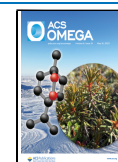
Table 1. Conventional Analyses of Coal Samples

sample	proximate analysis (wt %)			ultimate analysis (wt %, ad)					H/C
	M_{ad}	A_{ad}	V_{ad}	C	H	N	O	S	
CC	0.85	7.89	12.98	83.27	2.65	2.38	2.68	0.28	0.38
HJ	1.91	11.05	22.59	77.94	4.25	2.02	2.37	0.45	0.65
ST	1.52	4.94	22.25	82.73	4.40	0.66	5.30	0.45	0.64
NM	26.07	4.30	56.14	49.08	4.85	1.07	14.52	0.11	1.19

H_2O and mineral absorptions have a great interference effect on the O−H infrared absorption peak of coal.

Above all, there are still some problems to be solved in the study of OH groups in coal. First, the small sharp absorption in the wavenumber range of 3700−3590 cm^{-1} belongs to which O−H. Second, the content of O in coal is about 2−20% (mass content). The O-containing groups of coal include ether, ester, quinone, carboxyl, aldehyde, and so on. For coal with less than 10% O, the content of O−H should be small, so whether there will be a large number of hydrogen bonds. Theoretically, if there are no large number of hydrogen bonds, the broadened absorption peak near 3400 cm^{-1} will not appear. Third, when people use infrared spectroscopy, if the O−H peak is not analyzed, the interference of KBr−H_2O can be ignored. If the O−H peak is analyzed, there are usually three methods. One is to detect the O−H absorption peak of coal in a nitrogen atmosphere through in situ infrared spectroscopy. On the other hand, during the preparation of KBr tablets, vacuum drying is carried out at the same time to further remove the water absorbed by KBr during the sample preparation process; moreover, when studying the infrared spectrum of substances with OH groups in chemistry, the paraffin oil or fluorine oil grinding method is often used instead of the KBr pressing method. We can also use this method for reference in the infrared spectrum study of coal.

Therefore, in situ infrared, KBr pellet press, KBr pellet pressed drying, and paste methods were applied here to determine the influence of KBr crystal water and moisture contained in coal samples on the assignment of OH groups in coal. Furthermore, quantum chemistry theory was combined to simulate the infrared spectrum of phenols and alcohols in coal determined, so as to analyze the real infrared spectrum characteristics of organic OH groups in coal.

2. MATERIALS AND METHODS

2.1. Computational Details. There are mainly two types of OH in coals including alcohol O−H and phenol O−H. Few studies have found carboxylic acids in coal, so the O−H of carboxylic acids is not discussed in this paper. The molecular model of alcohol O−H and phenol O−H mainly uses the actual extracts existing in coals. According to the literature,[23−26] 1-undecanol, 2-methyl-3-biphenylmethanol, 2-undecanol, 1,2,3,4-tetrahydro-4-methylphenanthrene-1-ol, 2,4-dimethyl-2-pentanol, phenol, 2-naphthol, 2-hydroxyanthracene, pyren-10-ol, 1,2-benzopyrene-4-ol, and 2,4-di-*tert*-butyl-phenol are selected.

DFT provides an efficient way to quantitatively determine the electronic properties, geometries, and reaction energies. This promising method depends on its ability to consider electron exchange and correlation with acceptable computational cost. The IR spectrum of all molecules is therefore investigated by DFT at the level of B3LYP/6-31 G(d,p). Due to the error of the calculation method and the use of resonance approximation, the theoretical calculated infrared frequency

generally needs to be multiplied by the correction factor to be consistent with the experimental results. According to the literature,[27,28] the correction factor of B3LYP/6-31 G(d,p) calculation level is 0.9636. All the mentioned calculations are done with the Gaussian 16 suite of programs.[29]

2.2. Samples and Reagents. Four coal samples varying in rank from lignite to anthracite were collected from working faces of typical coal basins in China mining area, including Changchun (CC), Huajin (HJ), Sitai (ST), and Neimeng (NM). All the samples were crushed to pass through a 100-mesh sieve, followed by the conventional analyses. Proximate and ultimate analyses of the selected samples have been conducted, according the China National Standards GB/T 30732-2014, GB/T 476-2008, GB/T 214-2007, GB/T 19227-2008, and GB/T 31391-2015. Table 1 presents the analysis of coals. In order to prevent the interference of moisture in coal on the hydroxyl absorption peak in infrared spectrums, it should be dried in a 105 °C oven before the test and then let to cool (according to the national standard GB/T 30732-2014, the moisture in coal should be dried at 105−110 °C; finally, 105 °C is selected combined with the literature[23,30−33]).

The diluent used in the compression method of infrared spectrum experiment is KBr (spectral grade). KBr powder is easy to absorb moisture in the air, so it should be dried at 120 °C for 24 h and placed in a dryer for standby before use. The paste used in the paste method is Fluorolube, which is of reagent grade, and used without further purification.

2.3. FTIR Spectroscopy. *2.3.1. In Situ Infrared Experiment.* The infrared spectrum of coal samples was measured by a ThermoFisher iS50 infrared spectrometer. Under a nitrogen atmosphere, the temperature was increased to 100 °C at 5 °C/min and it was kept constant for 1 h (dry the coal sample to eliminate the interference of moisture on the O−H absorption peak). In situ DRIFT spectra of coal samples were recorded online.

2.3.2. KBr Pellet Press Method. Weigh 1 mg of the coal sample and 200 mg of spectral pure reagent potassium bromide (KBr) and place them in a grinding bowl. Under infrared light, the coal sample and KBr were fully mixed and ground with a grinding rod to make the average particle size under 2 μ. The ground mixture was evenly put into the mold, and then, the mold was put into the pressure gauge. Under the pressure of about 10 T/cm^2 for 2 min, a uniform translucent ingot was achieved. The infrared spectrum of coal samples was measured by a German BRUKER Fourier transform infrared spectrometer.

2.3.3. KBr Pellet Pressed Drying Method. The ground mixture (coal sample + KBr) was put into the mold, then the mold was put into the vacuum drying oven, and it was taken out after constant temperature of 100 °C for 1 h. Finally, it was cooled in the dryer and made into a uniform translucent ingot. The infrared spectrum of coal samples was measured by the German BRUKER Fourier transform infrared spectrometer.
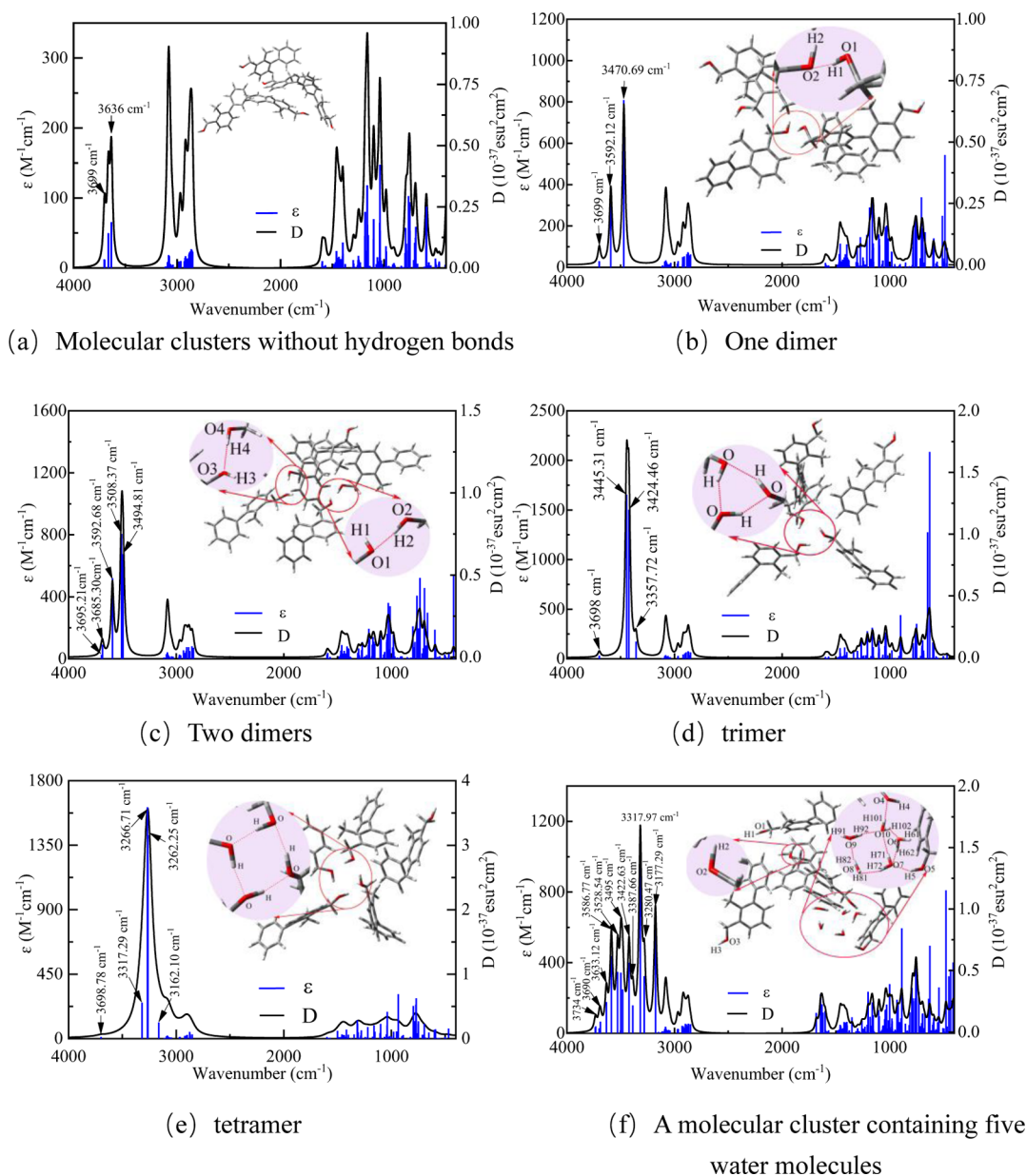
Figure 1. IR spectrum of substances containing O−H in coal.

2.3.4. Paste Method.[45,46] When preparing the sample, about 10 mg of the coal sample (without weighing) was taken and put into an agate grinding bowl. Half drop of Fluorolube was added, and the sample was ground into the average particle size under 2 μ with perfect mixing. The less the paste dosage, the better because the more the paste dosage, the stronger the paste absorption peak in the measured spectrum, the greater the impact. After grinding, the paste was scraped from the agate mortar with a hard plastic sheet and evenly coated between the two KBr crystal plates. KBr crystal plates shall be clamped on the fixture to measure the infrared spectrum of the coal sample.

3. RESULTS AND DISCUSSION

3.1. DFT Theoretical Analysis of Infrared Spectra of O−H. *3.1.1. Vibration Frequency and Intensity of O−H of*

(a) Molecular clusters without hydrogen bonds

(b) One dimer

(c) Two dimers

(d) trimer

(e) tetramer

(f) A molecular cluster containing five water molecules

Figure 2. Infrared spectra of five molecular clusters of 2-methyl-3-biphenylmethanol.

Organic Molecules. Each molecule of pure hydroxyl compound contains OH groups, and there must be a hydrogen bond between molecular clusters. The O−H stretching vibration peak becomes a broad large peak and moves toward low frequency. The chemical composition of coal is complex, and not every molecule has O−H. The content of O−H and the formation of the hydrogen bond directly affects the peak shape, peak position, and peak area of O−H stretching vibration wave of coal. Therefore, the infrared spectra of organic OH group-based compounds were analyzed by using quantum chemistry theory and Gaussian 16 software, as shown in Figure 1.

The O−H stretching vibration frequency of the selected five alcohol-hydroxy compounds appears in the range of 3699.04−3662.69 cm^{-1} (Figure 1). According to the infrared spectra of 1-undecanol, 2-undecanol, and 2,4-dimethyl-2-2-pentanol, the O−H stretching vibration frequency of them meets the rule of primary alcohol > secondary alcohol > tertiary alcohol. 2-

Methyl-3-methoxy-biphenyl is also a primary alcohol, and its O−H stretching vibration frequency is about 15.34 cm^{-1} higher than that of 1-undecanol. The reason is that its O atom is sp^2 hybrid, forming the O−H σ bond with a sp^2 hybrid orbital and the 1s orbital of the H atom; the C−O σ bond is formed by a sp^2 hybrid orbital and a sp^3 hybrid orbital of the connected methylene C atom; the other sp^2 hybrid orbit is occupied by a pair of unshared electrons. The p orbital occupied by the pair of solitary electrons that are not shared, and the π orbital of the aromatic ring cross each other on the side to form a p−πconjugate system. Due to the influence of the p−πconjugation effect, the O−H stretching vibration frequency shifts to higher wavenumber. However, the O−H and the benzene ring of 1,2,3,4-tetrahydro-4-methyl phenanthrol are not in the same plane, and the conjugation effect cannot be formed. 1,2,3,4-Tetrahydro-4-methyl phenanthrol and 2-undecanol are secondary alcohols, so their O−H stretching vibration frequency is similar.

The OH groups stretching vibration frequency of the selected six phenolic hydroxyl compounds appears in the range of 3703.37−3679.57 cm^{-1} (Figure 1). 2,4-Di-*tert*-butylphenol is affected by the ortho and para substituents, hindering the conjugation effect between the p orbital occupied by the lone pair electrons on the O atom and the π orbital of the aromatic ring, which makes the stretching vibration frequency of the phenolic hydroxyl O−H bond move to the direction of low wavenumber, 4.13 cm^{-1} lower than 1-undecanol. The stretching vibration frequency of the phenolic hydroxyl group without the influence of other substituents is not different from that of 1-undecanol, or slightly higher. In the hydroxyl stretching vibration, the vibration frequency of phenolic hydroxyl should be the highest. Because the O atom of the phenol hydroxyl group forms the C−O σ bond with a sp^2 hybrid orbital and a sp^2 hybrid orbital of the C atom on the benzene ring, the O−H σ bond is formed with a sp^2 hybrid orbital and the 1s orbital of the H atom; the other pair, which does not share the p orbital occupied by the solitary pair electrons, intersects with the π orbital of the aromatic ring to form a p−πconjugate system. Due to the influence of the p−πconjugation effect, the density of the electron cloud on the O atom shifts to the aromatic ring, which weakens the O−H bond and shifts the stretching vibration frequency of the hydroxyl group to the direction of high wavenumber.

Another characteristic infrared wave peak of more than 10 alcohols and phenols, C−O stretching vibration frequency, appears in the range of 1278.92−1026.46 cm^{-1} (Figure 1), and the C−OH bending vibration wave peak is in the range of 1470.12−136.83 cm^{-1}. In addition to C−O stretching vibration, it also includes C−C stretching, saturated C−H bending, unsaturated C−H bending, and Ar−H in-plane deformation vibration of the aromatic ring. These vibration frequencies are easy to cause coupling because they are located in the fingerprint area. The internal structure of the molecule has great influence, and the change rule is not as obvious as the O−H stretching vibration.

It can be seen from the above analysis that the stretching vibration of phenol and O−H containing the p−πconjugated system with π orbitals is about 3680−3690 cm^{-1}, the stretching vibration frequency of O−H of primary alcohol is about 3680 cm^{-1}, the stretching vibration frequency of secondary alcohol is about 3670 cm^{-1}, and the stretching vibration frequency of tertiary alcohol is about 3660 cm^{-1}. Meanwhile, the internal molecular structure factors such as the conjugation effect, steric hindrance, and hydrogen bond also affect the vibration frequency. The O−H stretching vibration frequency shifts to the direction of high wavenumber due to the conjugation effect; affected by steric hindrance, the intramolecular shifts to the direction of low wavenumber; affected by hydrogen bonding, it shifts to the direction of low wavenumber. However, the research results of C−O stretching vibration and C−OH bending vibration frequency are basically consistent with the results of existing organic spectrum textbooks[47,48] (C−O stretching vibration frequency appears in the range of 1278.92−1026.46 cm^{-1}, and C−OH bending vibration peak is in the range of 1470.12−136.83 cm^{-1}).

3.1.2. Effect of Hydrogen Bonding on the Vibration Frequency Migration of O−H.

In order to investigate the effect of intermolecular hydrogen bonding on the characteristic peaks of O−H infrared spectrum in coal, five 2-methyl-3-biphenylmethanol molecules are selected as examples for quantum chemistry calculation and analysis. It was found that five 2-methyl-3-biphenylmethanol molecules form molecular clusters through free combination, and there is no hydrogen bond between the five O−H, whose molecular configuration and infrared spectrum are shown in Figure 2a. The stretching vibration frequencies of the five O−H bases are 3702.40, 3699.55, 3699.09, 3664.06, and 3635.08 cm^{-1}, respectively.

As shown in Figure 2b, when the O−H of two of the five 2-methyl-3-biphenylmethanol molecules form hydrogen bonds with each other, its vibration frequency moves to the low-frequency direction with the telescopic vibration frequency of O2−H2 at 3592.12 cm^{-1} and O1−H1 at 3470.69 cm^{-1}. The frequencies of the other three O−H that do not form hydrogen bonds are 3699.54, 3699.20, and 3698.95 cm^{-1}, respectively.

As shown in Figure 2c, when the O−H of four of the five 2-methyl-3-biphenylmethanol molecules form hydrogen bonds, its vibration frequency moves toward low frequency, where 1O−1H is 3685.30 cm^{-1}, 2O−2H is 3508.37 cm^{-1}, 3O−3H is 3592.68 cm^{-1}, and 4O−4H is 3494.81 cm^{-1}; O−H without the hydrogen bond is 3695.21 cm^{-1}.

As shown in Figure 2d, when the three of the five 2-methyl-3-biphenylmethanol molecules form a trimer by hydrogen bonding, the other two molecules polymerize through van der Waals interaction. The stretching vibration frequencies of the two hydroxyl groups without hydrogen bonding are 3698.87 and 3698.84 cm^{-1}, respectively; the stretching vibration frequencies of the three hydroxyl groups forming hydrogen bonds are 3445.31, 3424.46, and 3357.72 cm^{-1}, respectively.

As shown in Figure 2e, when the four of the five 2-methyl-3-biphenylmethanol molecules form a tetramer by hydrogen bonding, the other molecule is polymerized by van der Waals interaction. The O−H stretching vibration frequency without hydrogen bonding is 3698.78 cm^{-1}; the O−H stretching vibration frequency of four hydrogen bonds is 3317.29, 3266.71, 3262.25, and 3162.10 cm^{-1}.

The above analysis shows that the 3700−3600 cm^{-1} region is the free O−H stretching vibration peak without hydrogen bonding. When 2-methyl-3-biphenylmethanol forms a dimer, trimer, and tetramer in the form of hydrogen bond, the OH base stretching vibration frequency moves to the low-frequency direction. The O−H stretching vibration frequency of the dimer hydrogen bond is about 3500 cm^{-1}; the O−H stretching vibration frequency of the trimer hydrogen bond is about 3430 cm^{-1}; the stretching vibration frequency of O−H forming the hydrogen bond of tetramer is about 3265 cm^{-1}.

3.1.3. Effect of Moisture on the O−H Vibration Spectrum of Coal.

In order to analyze the influence of hydrogen bonding between moisture molecules on O−H stretching vibration frequency in coal, five moisture molecules are added to the 2-methyl-3-biphenylmethyl molecular cluster, whose molecular configuration and infrared spectrum are shown in Figure 2f. The O−H stretching vibration of the molecular model includes the stretching vibration of the O−H of 2-methyl-3-biphenylmethyl and the stretching vibration of the O−H of moisture molecules. The stretching vibration of the O−H of 2-methyl-3-biphenylmethyl can be divided into the stretching vibration of the O−H without hydrogen bonding and the stretching vibration of the O−H with hydrogen bonding with moisture molecules. The O−H stretching vibration of moisture molecules can be divided into antisymmetric stretching vibration and symmetric stretching vibration. The hydrogen bond between moisture molecules and the hydrogen bond between moisture molecules and 2-methyl-3-biphenylmethanol
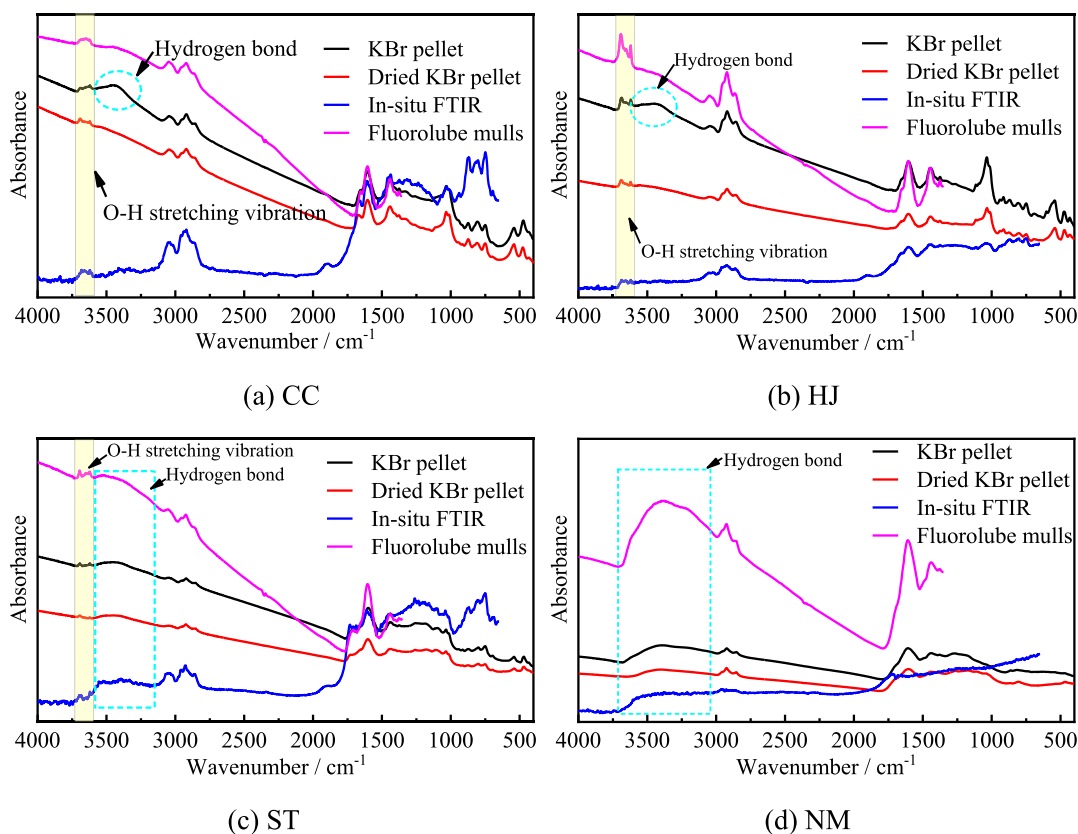
Figure 3. Infrared spectrum curve of coal samples measured by the KBr pellet pressed, KBr pellet pressed drying method, in situ infrared, and Fluorolube paste methods.

have different effects on the antisymmetric and symmetric stretching vibration frequencies.

In the molecular model, the non-hydrogen-bonded O−H of 2-methyl-3-biphenylmethanol are O1−H1, O2−H2, O3−H3 whose telescopic vibration frequencies are 3633.12, 3697.84, and 3698.99 cm^{-1}, respectively. O5−H5 is the donor of the hydrogen bond, and its stretching vibration frequency is 3481.97 cm^{-1}.

Geometric optimization and frequency calculation are conducted for moisture molecules. The theoretical value of O−H antisymmetric stretching vibration frequency is 3770.35 cm^{-1}, and the theoretical value of symmetric stretching vibration frequency is 3661.33 cm^{-1}. In the 2-methyl-3-biphenyl-methanol and moisture molecular cluster model, the two O−H of moisture molecule O6−H61 and O9−H91 do not form hydrogen bonds, and the antisymmetric stretching vibration frequency is 3736.28 and 3732.25 cm^{-1}, respectively; compared with the theoretical value, it decreased by 34.07−38.1 cm^{-1}. The O8−H81 of moisture molecule H81−O8−H82 also does not form hydrogen bonds, but the antisymmetric stretching vibration frequency was reduced to 3688.87 cm^{-1} due to space obstruction, which was 81.48 cm^{-1} lower than the theoretical value. As a hydrogen bond donor, the symmetric stretching vibration frequency of O8−H82 is 3387.66 cm^{-1}, which is 273.67 cm^{-1} lower than the theoretical value. Moisture molecules H71−O7−H72 form hydrogen bonds with moisture molecules H61−O6−H62, H81−O8−H82, H101−O10−H102, and O5−H5 of 2-methyl-3-biphenyl-methane, respectively. When O7−H71 is taken as a hydrogen bond donor, the antisymmetric stretching vibration is 3528.54 cm^{-1}. When O7−H72 is taken as the hydrogen bond donor,

the symmetric stretching vibration is 3177.29 cm^{-1}. Moisture molecules H101−O10−H102 form hydrogen bonds with moisture molecules H61−O6−H62, H71−O7−H72, H91−O9−H92, and O4−H4 of 2-methyl-3-biphenylmethane, respectively. When moisture molecule H101−O10−H102 is taken as the hydrogen bond donor, the antisymmetric telescopic vibration frequency of O−H is 3497.59 cm^{-1}, while the symmetrical telescopic vibration frequency is 3422.63 cm^{-1}. When moisture molecule H91−O9−H92 is taken as the hydrogen bond donor, the symmetric stretching vibration frequency of O9−H92 is 3317.97 cm^{-1}. When the moisture molecule H61−O6−H62 is taken as the hydrogen bond donor, the symmetric stretching vibration frequency of O6−H62 is 3280.47 cm^{-1}.

Above all, the O4−H4 hydroxyl group of 2-methyl-3-biphenylmethyl taken as the hydrogen bond receptor, which forms a hydrogen bond with the H$_2$O molecule, only decreased by 112.27 cm^{-1}, while the O5−H5 hydroxyl group of 2-methyl-3-biphenylmethyl as the hydrogen bond donor decreased by 217.07 cm^{-1}, showing that the hydrogen bond has greater influence on the donor hydroxyl stretching vibration frequency. Moisture molecules H71−O7−H72 and H101−O10−H102 form four hydrogen bonds with surrounding molecules, respectively. Due to the different intermolecular arrangement, the hydroxyl stretching vibration frequency decreased by 484.04 cm^{-1} at most. Moisture molecules H61−O6−H62, H81−O8−H82, and H91−O9−H92 form two hydrogen bonds with surrounding molecules, respectively. The moisture molecule H61−O6−H62 is located in the ternary ring, and the symmetrical stretching vibration frequency of −OH is reduced by 380.86 cm^{-1}. The moisture

molecules H81−O8−H82 and H91−O9−H92 are located in the quaternary ring, and the symmetrical stretching vibration frequency of −OH is reduced by 343.36 cm^{-1}. The hydrogen bond between moisture molecules reduces the symmetry stretching vibration of O−H more. The reduction of the symmetric stretching vibration frequency of the O−H of the hydrogen bond donor in the ternary ring is greater than that of the O−H of the hydrogen bond donor in the quaternary ring. Under the action of hydrogen bond, the maximum frequency intensity of O−H stretching vibration of the moisture molecule is 3317.97 cm^{-1}.

3.2. Experimental Analysis of the O−H Stretching Vibration Spectrum in Coal.

3.2.1. Comparison of Infrared Spectra of KBr Pellet Press, In Situ Infrared, and Paste. The infrared spectrum curves of coal samples measured by KBr pellet pressed, KBr pellet pressed drying, in situ infrared, and Fluorolube paste methods are shown in Figure 3. In theory, KBr has no absorption peak at 400−4000 cm^{-1}. The infrared spectra of four kinds of coal samples measured by the KBr pellet pressed method form a broad wave peak at 3440 cm^{-1}. However, the infrared spectra of CC and HJ coal samples measured by the KBr pellet pressed drying, in situ infrared, and Fluorolube oil paste methods showed that the O−H in these two coals did not form hydrogen bonds, indicating that the KBr gasket contains hydrogen bonds. In this paper, the infrared spectrum of the KBr gasket was detected separately and compared with the infrared spectrum of HJ coal sample. As shown in Figure 4, the infrared spectrum of pure KBr shows
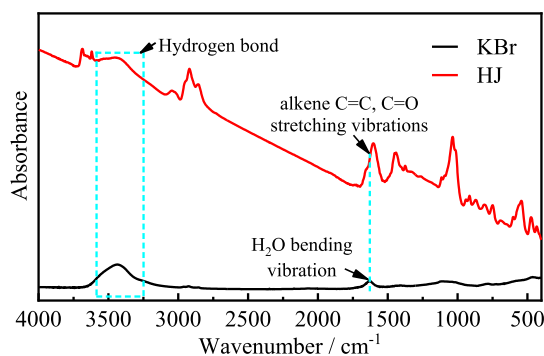

Figure 4. Infrared spectrum of KBr and HJ coal samples measured by the KBr pellet pressed method.

obvious peaks near 3400 and 1633 cm^{-1}, caused by KBr absorbing a certain amount of moisture during the grinding and pressing process. When testing the infrared spectrum of coal samples, these two peaks have great interference on the analysis of −OH, olefin C=C bond, and C=O bond stretching vibration in coal. Finally, we found that the KBr pellet pressed drying effect is better.

The peaks of O−H base stretching vibration measured by the KBr pellet pressed drying, in situ infrared, and Fluorolube paste methods are basically the same, which can eliminate the interference of KBr hydrophobicity on infrared spectra. The stability of the infrared spectrum signal detected by in situ infrared detection is the worst, and the experimental cost is the highest. The infrared spectrum signal measured by the Fluorolube paste method has good stability and high intensity, but it can only analyze the functional groups of 4000−1350 cm^{-1}, and the functional groups between 1350 and 400 cm^{-1} need to be measured by the Nujol paste method. The infrared spectrum signal intensity measured by the dried KBr pellet pressed method is relatively low, but it does not affect the experimental effect.

3.2.2. OH Groups' Infrared Spectrum Analysis of Deashing Coal. In order to analyze and quantify the infrared spectrum characteristics of organic O−H in coal, it is necessary to exclude the influence of mineral crystal moisture. Therefore, four kinds of coal samples were deashed, and the infrared spectrum of the dried deashing coal was detected by the KBr pellet pressed drying method. The infrared spectra of four kinds of deashing coal after baseline correction are shown in Figure 5.

It can be seen from Figure 5 that CC, HJ, and ST coal samples still have multiple overlapping peaks between 3720 and 3690 cm^{-1}; there is no hydrogen bond in CC and HJ coal molecules; a small amount of hydrogen bonds were formed in ST coal molecules; a large number of hydrogen bonds are formed in NM coal molecules. After deashing, the peak position of the hydroxyl stretching vibration of the coal sample does not change, and the absorbance basically does not change, explaining that the infrared spectrum characteristics of coal samples are basically not affected by mineral crystal moisture.

3.2.3. Infrared Spectrum Characteristics of −OH in Coal. The oxygen content of CC and HJ coal samples is less than 3% (Table 1), and the O−H stretching vibration peak is at 3713−3600 cm^{-1} (Figure 5). According to the peak position, peak strength, and oxygen element content of O−H stretching

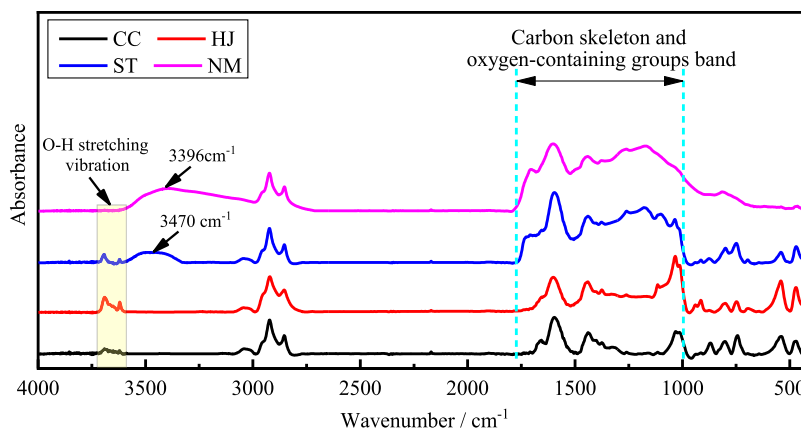**Figure 5.** Infrared spectrum of the deashing coal sample measured by the KBr pellet pressed method after vacuum heating.
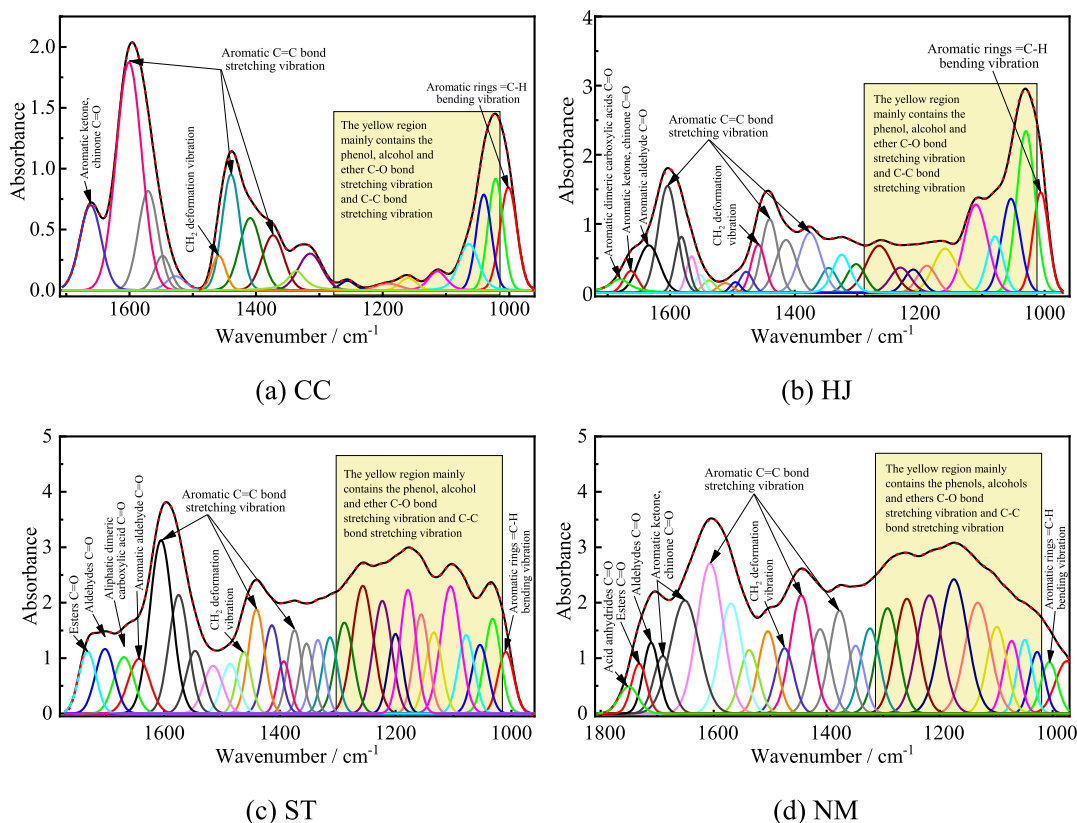
(a) CC

(b) HJ

(c) ST

(d) NM

Figure 6. Spectral band peak fitting curve at 1800−1000 cm^{-1} of the infrared spectrum of coal samples.

vibration, it can be determined that CC and HJ coal samples basically do not form hydrogen bonds.

The O−H-based stretching vibration peak of the ST coal sample (oxygen content 5.3%) is located at 3718−3326 cm^{-1} (Figure 5), which is divided into two parts. One is composed of several overlapping small and sharp peaks, located at 3718−3606 cm^{-1}, which belong to the free O−H stretching vibration peak; the other is a relatively broad peak, located at 3606−3326 cm^{-1}, with the peak center at 3470 cm^{-1}. The peak shape is relatively symmetrical, belonging to the O−H stretching vibration peak of the hydrogen bond. ST coal samples have relatively high oxygen content, and some O−H form hydrogen bonds. According to the theoretical analysis of the effect of hydrogen bond on O−H stretching vibration frequency, the hydrogen bond in the ST coal sample is mainly a trimer.

The oxygen content of the NM coal sample is 14.52%, which is the highest among the four coal samples. As displayed in Figure 5, the O−H stretching vibration peak and the stretching vibration peak of the aromatic C−H bond overlap each other to form a broad wave peak (located at 3625−3000 cm^{-1}), with the peak center at 3396 cm^{-1}. Its peak shape is asymmetrical, and the half peak width in the high frequency direction is narrow, and the half peak width in the low-frequency direction is wide. According to the theoretical analysis results of the influence of the hydrogen bond on the O−H stretching vibration frequency, the hydrogen bond dimer, trimer, and tetramer in the NM coal sample are all present, and the content of the tetramer is relatively high, which leads to the asymmetry of the O−H stretching vibration peak. It can be seen from Figure 2a−e that the O−H stretching vibration intensity after the formation of the hydrogen bond increases by about 10−100 times. The sensitivity of the infrared spectrum

experimental instrument is limited. When there are a large number of hydrogen bonds, it is very difficult to detect a very small amount of free O−H radical stretching vibration peaks.

As exhibited in Figure 5, the infrared spectrum of coal roughly contains three spectral bands, which are the O−H stretching vibration peak at 3730−3100 cm^{-1}, the C−H bond telescopic vibration peak at 3100−2760 cm^{-1}, and the spectral band at 1800−400 cm^{-1} that can be divided into two segments (one is the carbon skeleton and oxygen-containing functional group region at 1800−1000 cm^{-1}; the other is the benzene substitution region at 1000−400 cm^{-1}).

The chemical composition of coal is complex, and the main components are aromatic hydrocarbons and aliphatic hydrocarbons (composed of C/H/O/N/S five elements). The infrared peaks of various functional groups between 1800 and 1000 cm^{-1} of the coal sample overlap with each other, forming a relatively wide spectral band. On the basis of the analysis on the vibration frequency and intensity of organic molecule O−H and the description in the literature, C−OH in-plane bending vibration is within the range of 1500−1350 cm^{-1}; C−OH telescopic vibration belongs to the strong absorption zone, located in the range of 1280−1000 cm^{-1}. In order to combine the C−O stretching vibration peak and C−OH in-plane bending vibration, further analysis of the hydroxyl infrared spectrum, PeakFit has been applied to conduct peak-splitting processing for spectral band at 1800−1000 cm^{-1} according to the second derivative spectrum method, as shown in Figure 6.

The bending vibration wavenumber in the C−OH plane is in the range of 1500−1350 cm^{-1}, and the bending vibration wavenumber in the C−OH plane of different hydroxyl compounds varies greatly. For example, the C−OH in-plane bending vibration wavenumbers of pyren-10-ol, 1-undecanol,
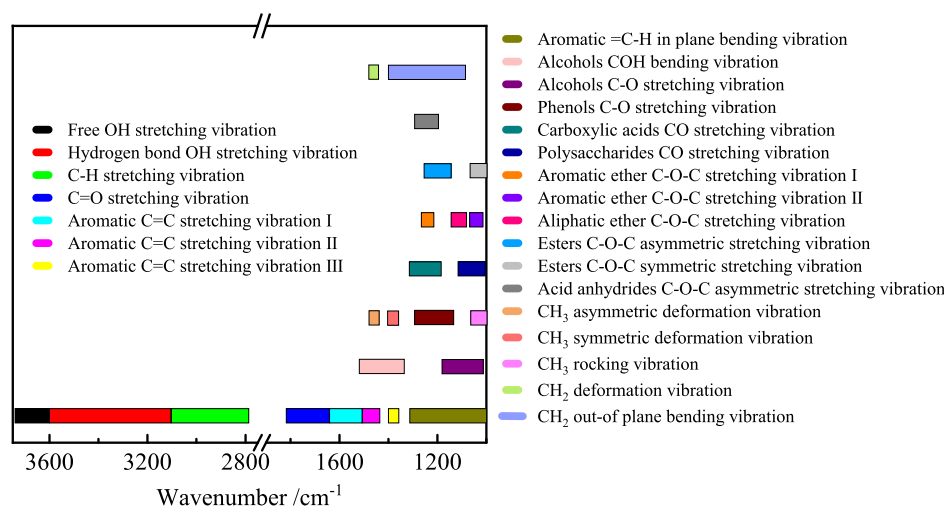
Figure 7. Infrared spectrum distribution of coal functional groups.
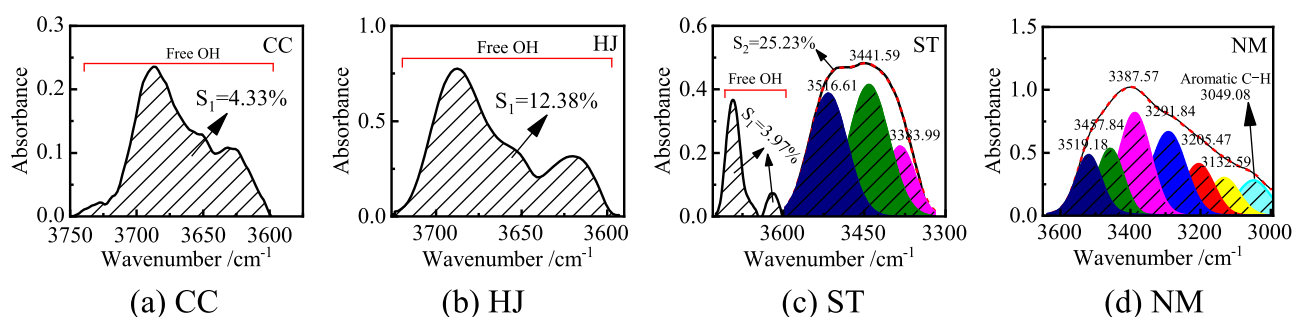

Figure 8. O−H stretching vibration peak of coal samples.

2-methyl-3-biphenylmethanol, and 1,2,3,4-tetrahydro-4-methylphenanthrene-1-ol are 1455.69, 1417.00, 1398.48, and 1383.45 cm^{-1}, respectively. In the 1500−1350 cm^{-1} spectral band of the infrared spectrum of coal, the C═C stretching vibration of aromatic hydrocarbon also has two vibration peaks in this spectral band (1500−1450 cm^{-1} and 1380 ± 10 cm^{-1}, respectively). It can be seen from Figure 6 that the aromatic hydrocarbon C═C of the four coal samples has high tensile vibration intensity and high characteristics, covering the bending vibration peak in the C−OH plane.

The C−O stretching vibration of alcohol/phenol (in the range of 1280−1000 cm^{-1}) is also disturbed by other functional groups. The coal molecules are mainly aromatic compounds and contain a certain amount of aromatic ═C−H bonds. When the number of substituents and the position of substituents on the aromatic ring are different, there are several absorption bands in the bending vibration of the ═C−H plane in the range of 1300−990 cm^{-1}. The polar substituents can significantly enhance these absorption peaks, which are superimposed with the C−O stretching vibration peaks of alcohol/phenol and cannot be identified. At the same time, the C−O stretching vibration of ether also overlaps with the C−O stretching vibration band of alcohol/phenol. The antisymmetric stretching vibration wavenumber of saturated fatty ether C−O−C is between 1125 and 1110 cm^{-1}. The antisymmetric and symmetric stretching vibrations of aromatic ether are located near 1240 ± 10 and 1040 ± 10 cm^{-1}, respectively. By summarizing a large number of experiments and literature studies, the infrared spectrum distribution of coal functional groups was drawn (Figure 7).

Figure 7 shows that the 1500−1000 cm^{-1} spectral band of the coal infrared spectrum involves complex functional groups and is not suitable for auxiliary analysis of OH groups characteristics. The 3730−3100 cm^{-1} spectral band is not interfered by other functional groups and is most suitable for analyzing the characteristics of OH groups in coal. However, when collecting experimental data, attention should be paid to eliminating moisture interference.

3.3. Quantitative Analysis of O−H in Coal. *3.3.1. Analysis of Oxygen Content in Coal.* The content of organic oxygen elements in coal must be determined before the quantitative analysis of O−H in coal. According to the element analysis (Table 1), the oxygen element content of CC, HJ, ST, and NM coal samples is 2.68, 2.37, 5.30, and 14.52% respectively. When the mass content of elements in coal samples is converted into atomic content, the number of oxygen atoms per 100 atoms in CC, HJ, ST, and NM coal samples is 1.69, 1.54, 3.02, and 7.96 respectively.[34−41]

According to the infrared spectrum of coal samples (Figure 5), the O−H in CC and HJ coal with oxygen content less than 3% does not form hydrogen bonds. The O−H in ST coal with 5.30% oxygen content forms a small amount of hydrogen bonds. The oxygen content of NM coal is the best, and its infrared spectrum has the largest stretching vibration peak of hydrogen bond O−H, which moves to about 3400 cm^{-1} in the low-frequency direction, and the right side of the peak overlaps with the stretching vibration peak of the aromatic C−H bond.[42−44]

In addition to the OH group, the oxygen-containing functional groups in coal also include ether (C−O−C), C═

Table 2. Peak Area of O−H Stretching Vibration Wave of Coal Samples

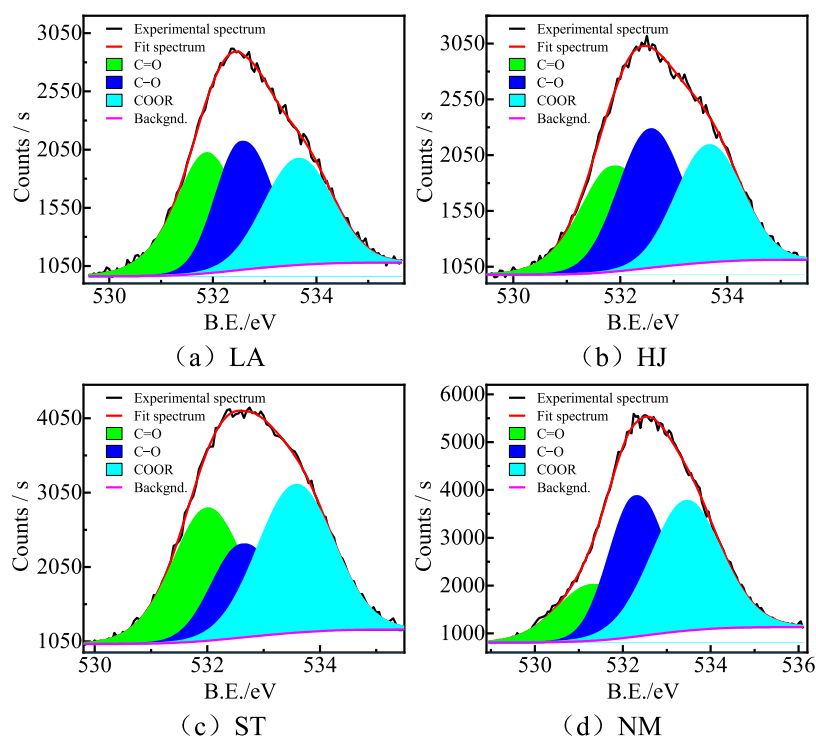|	CC		HJ		ST		NM	
	peak position	peak area (%)	peak position	peak area (%)	peak position	peak area (%)	peak position	peak area (%)
free OH(S1) hydrogen bond OH(S$_2$)	3750−3600	4.33	3725−3600	12.38	3725−3600	3.97	3750−3600	0.00
					3516.61	9.75	3519.18	14.02
					3441.59	11.05	3457.84	14.37
					3383.99	4.44	3387.57	26.40
							3291.84	23.37
							3205.47	12.64
							3132.59	9.20
total		4.33		12.38		29.20		100.00

Figure 9. XPS fine spectrum of oxygen element of coal samples.

O, COOR, and so on. Compared with the relative content of O−H in different coal samples, semi-quantitative analysis can be carried out by the infrared spectrum peak height and peak area.

3.3.2. Quantitative Determination of O−H in Coal by Infrared Spectroscopy. There are two methods for quantitative analysis of the infrared spectrum: one is to measure the peak height of the absorption peak, that is, to measure the absorbance of the absorption peak; the other is to measure the peak area of the absorption peak. Quantitative analysis using the peak area is often more accurate than quantitative analysis using peak height.

There are many kinds of O−H compounds in coal, and the O−H base peaks are overlapped by many sub-peaks, forming an asymmetric absorption band (Figure 8). The O−H absorption band is divided into two sections, one is the free O−H stretching vibration band (between 3750 and 3600 cm^{-1}), that is, the O−H stretching vibration band without hydrogen bonds; the other is a broad O−H stretching vibration band with hydrogen bonds, and the infrared spectrum is between 3600 and 3100 cm^{-1}.

According to the theoretical analysis, the tensile vibration intensity of the O−H base increases by about 10−100 times due to the hydrogen bond effect. Therefore, the quantity of the free O−H group and the hydrogen bond O−H group need to be compared separately. The free O−H group is directly quantitatively analyzed by peak area comparison. For the broad stretching vibration peak of hydrogen bonding O−H, the peak position, peak height, peak area, and peak shape have high reference value for the quantification of the hydrogen bonding O−H group.[48,49]

In order to quantitatively analyze the content of t hehydrogen bond O−H in ST and NM coal samples, the broad O−H stretching vibration wave peak was fitted by peak division to determine the peak position, peak height, and peak area of each sub-peak. The O−H stretching vibration peak of hydrogen bonds of the ST coal sample is fitted with three sub-peaks, which are 3516.61, 3441.59, and 3383.99 cm^{-1}, respectively (Figure 8c). The O−H stretching vibration peak of hydrogen bonds of the NM coal sample is fitted with six sub-peaks, which are 3519.18, 3457.84, 3387.57, 3291.84, 3205.47, and 3132.59 cm^{-1}, respectively (Figure 8d). Combined with the analysis of quantum chemistry theory,

when the hydroxyl compound exists as a dimer, the O−H stretching vibration peak is at 3500 ± 30 cm^{-1}, and the half peak width in the high-frequency direction is large; when the hydroxyl compound exists as a trimer, the O−H stretching vibration peak is at 3430 ± 10 cm^{-1}, and the peak shape is symmetrical; when the hydroxyl compound exists as a tetramer, the O−H stretching vibration peak is at 3265 ± 5 cm^{-1}, and the peak shape is symmetrical; when a number of moisture molecules and hydroxyl compounds form a polymer, the O−H stretching vibration peak is located at 3318 cm^{-1}, and the half peak width in the high-frequency direction is large. The O−H stretching vibration peak of hydrogen bonds in the ST coal sample is located near 3450 cm^{-1}, and the peak shape is symmetrical, indicating that the O−H in the ST coal sample is mainly dimers and trimers.

The O−H stretching vibration peak area of each coal sample according to the peak division results is as shown in Table 2. For the following coal samples, the O−H base stretching vibration infrared peak area of NM coal samples is taken as the control group.

The free O−H stretching vibration peak areas of the three coal samples of CC/HJ/ST are 4.33, 12.38, and 3.97%, respectively. The content of free O−H in the ST coal sample is lower than CC and HJ but some O−H form hydrogen bonds. The area of the hydrogen bond O−H stretching vibration peak of the ST coal sample only accounts for 25.24% of the NM coal sample. The O−H content of the NM coal sample should be the largest of the four coal samples. The comparison of O−H content of HJ and ST coal samples also needs to be combined with XPS experiment for auxiliary analysis.

3.3.3. Quantification of O−H-Based XPS in Coal. According to the organic element analysis of coal samples, the oxygen element content has been determined. Combined with XPS fine spectrum of oxygen elements, the oxygen content of three chemical forms of C−O, C=O, and COOR in coal samples can be further quantified. Among them, C−O functional groups include C−OH and C−O−C. Therefore, the content of oxygen in O−H of coal is definitely lower than the content of C−O functional group determined by XPS oxygen element fine spectrum.

Figure 9 shows the narrow energy spectrum of O 1s of coal samples. The O 1s peak curves were fitted using the Gaussian line shape, and divided into three peaks, which are 531.7 ± 0.3, 532.5 ± 0.2, and 533.5 ± 0.2 eV, respectively. The spectrum confirmed the presence of C=O (carbonyl), C−O (alcohol, phenol, or ether), and COOR (ester) in coal samples.

According to the peak fitting results of energy spectrum data, the contents of oxygen-containing functional groups in coal were calculated, as shown in Figure 10. The order of C−O (alcohol, phenol or ether) contents in coal samples from high to low was NM (5.47%) > ST (1.14%) > HJ (0.87%) = CC (0.87%).

The above analysis shows that the O−H content of CC and HJ coal samples is not higher than 0.87%; the O−H content in the ST coal sample is not higher than 1.14%; and the O−H content of the NM coal sample is not higher than 5.47%. According to the quantitative analysis of infrared spectrum, the O−H content in CC is lower than that in HJ, indicating that the ether content of the CC coal sample is higher than that of the HJ coal sample.
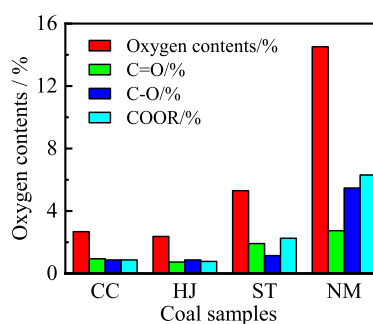

Figure 10. Content of oxygen element and various chemical forms in coal samples.

4. CONCLUSIONS

The infrared spectrum characteristics of O−H in coal are discussed through infrared spectrum experiment and quantum chemistry theory, and the quantitative analysis of O−H is assisted by XPS experiment. The conclusions are as follows.

(1) After DFT calculation, it was found that the free O−H radical stretching vibration peak without hydrogen bonding was located between 3700 and 3600 cm^{-1}. After the O−H radicals form hydrogen bonds with each other, the O−H radical stretching vibration frequency moves toward the low frequency direction, and the lower the wavenumber, the more the OH radical content.

(2) The OH based absorption spectrum in coal is divided into two sections, one of which is a free O−H based stretching vibration spectrum (located between 3750 and 3600 cm^{-1}) with sharp small peaks; when the content of OH group in coal exceeds a certain limit, hydrogen bonds are formed between molecules. From the formation of a broad hydrogen bond O−H stretching vibration band (located between 3600 and 3100 cm^{-1}), the larger the hydrogen bond content, the more the wavenumber, and the peak position can move to about 3400 cm^{-1}.

(3) The O−H based stretching vibration peak (3730−3100 cm^{-1} spectral band) in coal is not interfered by other functional groups and is more suitable for analyzing the O−H based characteristics of coal, which can be used as a basis for comparative analysis of relative content.

(4) The O−H stretching vibration peaks of the infrared spectra measured by dry potassium bromide tablets, in situ infrared spectroscopy, and the Fluorolube oil paste method are basically consistent, which can eliminate the interference of KBr hydrophobicity on the infrared spectra.

■ AUTHOR INFORMATION

Corresponding Author

Fengwei Dai − *College of Safety Science & Engineering, Liaoning Technical University, Fuxin, Liaoning 123000, China;* ⊙ orcid.org/0000-0003-0609-7766; Email: daifengwei214@163.com

Authors

Qiuying Zhuang − *College of Safety Science & Engineering, Liaoning Technical University, Fuxin, Liaoning 123000, China;* ⊙ orcid.org/0009-0005-8404-9278

Ge Huang − *College of Safety Science & Engineering, Liaoning Technical University, Fuxin, Liaoning 123000, China*

Hanzhong Deng − *College of Materials Science & Engineering, Liaoning Technical University, Fuxin, Liaoning 123000, China*

Xun Zhang − *College of Mining, Liaoning Technical University, Fuxin, Liaoning 123000, China*

Complete contact information is available at:
https://pubs.acs.org/10.1021/acsomega.3c01336

Notes

The authors declare no competing financial interest.

■ REFERENCES

(1) Painter, P. C.; Snyder, R. W.; Starsinic, M.; Coleman, M. M.; Kuehn, D. W.; Davis, A. Concerning the application of FT-IR to the study of coal: a critical assessment of band assignments and the application of spectral analysis programs. *Appl. Spectrosc.* **1981**, *35*, 475−485.

(2) Painter, P. C.; Snyder, R. W.; Starsinic, M.; Coleman, M. M.; Kuehn, D. W.; Davis, A. Fourier Transform IR Spectroscopy: Application to the Quantitative Determination of Functional Groups in Coal. *ACS Symp. Ser.* **1982**, *205*, 47−76.

(3) Chen, C.; Gao, J.; Yan, Y. Observation of the type of hydrogen bonds in coal by FTIR. *Energy Fuel.* **1998**, *12*, 446−449.

(4) Miura, K.; Mae, K.; Li, W.; Kusakawa, T.; Morozumi, F.; Kumano, A. Estimation of hydrogen bond distribution in coal through the analysis of OH stretching bands in diffuse reflectance infrared spectrum measured by in-situ technique. *Energy Fuel.* **2001**, *15*, 599−610.

(5) Machnikowska, H.; Krztoń, A.; Machnikowski, J. The characterization of coal macerals by diffuse reflectance infrared spectroscopy. *Fuel* **2002**, *81*, 245−252.

(6) Li, D.; Li, W.; Li, B. A new hydrogen bond in coal. *Energy Fuel.* **2003**, *17*, 791−793.

(7) Tao, L. D.; Wen, L.; Qing, L. B. 04/01189 Hydrogen bonds in coal. The influence of coal rank and the recognition of a new hydrogen bond in coal. *Fuel Energy Abstr.* **2004**, *45*, 164.

(8) Chen, Y.; Mastalerz, M.; Schimmelmann, A. Characterization of chemical functional groups in macerals across different coal ranks via micro-FTIR spectroscopy. *Int. J. Coal Geol.* **2012**, *104*, 22−33.

(9) Solomon, P. R.; Carangelo, R. M. FT-i.r. analysis of coal. *Fuel* **1988**, *67*, 949−959.

(10) Xuguang, S. The investigation of chemical structure of coal macerals via transmitted-light FT-IR microspectroscopy. *Spectrochim. Acta, Part A* **2005**, *62*, 557−564.

(11) Choperena, A.; Painter, P. An infrared spectroscopic study of hydrogen bonding in ethyl phenol: A model system for polymer phenolics. *Vib. Spectrosc.* **2009**, *51*, 110−118.

(12) Geng, W.; Nakajima, T.; Takanashi, H.; Ohki, A. Analysis of carboxyl group in coal and coal aromaticity by Fourier transform infrared (FT-IR) spectrometry. *Fuel* **2009**, *88*, 139−144.

(13) Sonibare, O. O.; Haeger, T.; Foley, S. F. Structural characterization of Nigerian coals by X-ray diffraction, Raman and FTIR spectroscopy. *Energy* **2010**, *35*, 5347−5353.

(14) Balachandran, M. Role of infrared spectroscopy in coal analysis—an investigation. *Am. J. Anal. Chem.* **2014**, *05*, 367−372.

(15) Qin, Z.-H.; Chen, H.; Yan, Y.-J.; Li, C.-S.; Rong, L.-M.; Yang, X.-Q. FTIR quantitative analysis upon solubility of carbon disulfide/N-methyl-2-pyrrolidinone mixed solvent to coal petrographic constituents. *Fuel Process. Technol.* **2015**, *133*, 14−19.

(16) He, X.; Liu, X.; Nie, B.; Song, D. FTIR and Raman spectroscopy characterization of functional groups in various rank coals. *Fuel* **2017**, *206*, 555−563.

(17) Cui, X.; Li, X.; Li, Y.; Li, S. Evolution mechanism of oxygen functional groups during pyrolysis of Datong coal. *J. Therm. Anal. Calorim.* **2017**, *129*, 1169−1180.

(18) Xiong, G.; Li, Y.; Jin, L.; Hu, H. In situ FT-IR spectroscopic studies on thermal decomposition of the weak covalent bonds of brown coal. *J. Anal. Appl. Pyrolysis* **2015**, *115*, 262−267.

(19) Xin, H.-h.; Wang, D.-m.; Qi, X.-y.; Qi, G.-s.; Dou, G.-l. Structural characteristics of coal functional groups using quantum chemistry for quantification of infrared spectra. *Fuel Process. Technol.* **2014**, *118*, 287−295.

(20) Choi, H.; Jo, W.; Kim, S.; Yoo, J.; Chun, D.; Rhim, Y.; Lim, J.; Lee, S. Comparison of spontaneous combustion susceptibility of coal dried by different processes from low-rank coal. *Korean J. Chem. Eng.* **2014**, *31*, 2151−2156.

(21) Solomon, P. R.; Carangelo, R. M. FTIR analaysis of coal. 1. techniques and determination of hydroxyl concentrations. *Fuel* **1982**, *61*, 663−669.

(22) Okolo, G. N.; Neomagus, H. W.; Everson, R. C.; Roberts, M. J.; Bunt, J. R.; Sakurovs, R.; Mathews, J. P. Chemical-structural properties of South African bituminous coals: Insights from wide angle XRD-carbon fraction analysis, ATR-FTIR, solid state 13C NMR, and HRTEM techniques. *Fuel* **2015**, *158*, 779−792.

(23) Sharma, D. K.; Dhawan, H.; Morgan, T.; Crocker, M. Py-GCMS studies of Indian coals and their solvent extracted products. *Fuel* **2019**, *256*, 115981.

(24) Fan, X.; Wei, X.-Y.; Zong, Z.-M. Application of gas chromatography/mass spectrometry in studies on separation and identification of organic species in coals. *Fuel* **2013**, *109*, 28−32.

(25) Zong, Y.; Zong, Z.-M.; Ding, M.-J.; Zhou, L.; Huang, Y.-G.; Zheng, Y.-X.; Jin, X.; Ma, Y.-M.; Wei, X.-Y. Separation and analysis of organic compounds in an Erdos coal. *Fuel* **2009**, *88*, 469−474.

(26) Yang, Z.; Fu, L.; Fan, F. Thermal Characteristics and Kinetics of Waste Camellia oleifera Shells by TG−GC/MS. *ACS Omega* **2019**, *4*, 10370−10375.

(27) Kesharwani, M. K.; Brauer, B.; Martin, J. M. L. Frequency and zero-point vibrational energy scale factois for double-hybrid density functionals (and other selected methods): Can anharmonic force fields be avoided? *J. Phys. Chem. A* **2015**, *119*, 1701−1714.

(28) Wong, M. W. Vibrational frequency prediction using density functional theory. *Chem. Phys. Lett.* **1996**, *256*, 391−399.

(29) Frisch, M. J.; Trucks, G. W.; Schlegel, H. B.; Scuseria, G. E.; et al. *Gaussian 16* revision a. 03; Gaussian. Inc., 2016.

(30) Sun, Y.; Wang, X.; Feng, T.; Yu, G.; Wang, F. Evaluation of coal extraction with supercritical carbon dioxide/1-methyl-2-pyrrolidone mixed solvent. *Energy Fuel.* **2014**, *28*, 816−824.

(31) Feng, L.; Zhao, G.; Zhao, Y.; Zhao, M.; Tang, J. Construction of the molecular structure model of the Shengli lignite using TG-GC/MS and FTIR spectrometry data/MS and FTIR spectrometry data. *Fuel* **2017**, *203*, 924−931.

(32) Ni, H.; Yan, L.; Ma, C.; Xu, C.; Shi, Q. Molecular composition of soxhlet N-Methyl-2-pyrrolidone extracts from a lignite. *Energy Fuel.* **2016**, *30*, 9285−9292.

(33) Wang, J.; He, Y.; Li, H.; Yu, J.; Xie, W.; Wei, H. The molecular structure of Inner Mongolia lignite utilizing XRD, solid state 13C NMR, HRTEM and XPS techniques. *Fuel* **2017**, *203*, 764−773.

(34) Zhang, Y.; Zhang, J.; Li, Y.; Gao, S.; Yang, C.; Shi, X. Oxidation characteristics of functional groups in relation to coal spontaneous combustion. *ACS Omega* **2021**, *6*, 7669−7679.

(35) Miura, K.; Mae, K.; Li, W.; Kusakawa, T.; Morozumi, F.; Kumano, A. Estimation of hydrogen bond distribution in coal through the analysis of OH stretching bands in diffuse reflectance infrared spectrum measured by in-situ technique. *Energy Fuels* **2001**, *15*, 599−610.

(36) Gao, Y.; Lei, H.; Yin, X.; Zhang, Y.; Huang, Z.; Yin, Y.; Xiao, S.; Wang, P. Study of the Change Laws of Free Radicals and Functional Groups during Coal Oxidation. *ACS Omega* **2023**, *8*, 7102−7110.

(37) Feng, Z.-H.; Liu, L.; Mo, W.-L.; Wei, X.-Y.; Yuan, J.-R.; Fan, X.; Niu, J.-M. Copyrolysis and Cocombustion Performance of Karamay

Oily Sludge and Zhundong Subbituminous Coal. *ACS Omega* **2022**, *7*, 43793−43802.

(38) Zhong, X.; Jian, H.; Dou, G.; Liu, J.; Tan, H. Preparation and Characterization of a Bentonite-Based Hybrid Gel for Coal Spontaneous Combustion Prevention. *ACS Omega* **2022**, *7*, 46536−46549.

(39) Zheng, Y.; Li, S.; Jiang, B.; Yu, G.; Ren, B.; Zheng, H. One-Step Preparation of Activated Carbon for Coal Bed Methane Separation/ Storage and Its Methane Adsorption Characteristics. *ACS Omega* **2022**, *7*, 45107−45119.

(40) Gonjo, T.; Futami, Y.; Morisawa, Y.; Wojcik, M. J.; Ozaki, Y. Hydrogen bonding effects on the wavenumbers and absorption intensities of the OH fundamental and the first, second, and third overtones of phenol and 2, 6-dihalogenated phenols studied by visible/near-infrared/infrared spectroscopy. *J. Phys. Chem. A* **2011**, *115*, 9845−9853.

(41) Kou, J.; Bai, Z.; Li, W.; Bai, J.; Guo, Z. Effects of aromatic solvents and temperature on rearrangement of hydrogen bonds in brown coals. *Energy Fuel.* **2013**, *27*, 6419−6429.

(42) Liu, S. M.; Li, X. Experimental study on the effect of cold soaking with liquid nitrogen on the coal chemical and microstructural characteristics. *Environ. Sci. Pollut. Res.* **2022**, *30*, 36080−36097.

(43) Liu, S. M.; Sun, H.; Zhang, D.; Yang, K.; Wang, D.; Li, X.; Long, K.; Li, Y. Nuclear magnetic resonance study on the influence of liquid nitrogen cold soaking on the pore structure of different coals. *Phys. Fluids* **2023**, *35*, 012009.

(44) Zhang, L.; Shen, W.; Li, X.; Wang, Y.; Qin, Q.; Lu, X.; Xue, T. Abutment pressure distribution law and support analysis of super large mining height face. *Int. J. Environ. Res. Publ. Health* **2022**, *20*, 227.

(45) Zhang, L.; Shen, W.; Li, X.; Wang, Y.; Qin, Q.; Lu, X.; Xue, T. Abutment pressure distribution law and support analysis of super large mining height face. *Int. J. Environ. Res. Publ. Health* **2022**, *20*, 227.

(46) Wang, S.; Li, X.; Qin, Q. Study on surrounding rock control and support stability of Ultra-large height mining face. *Energies* **2022**, *15*, 6811.

(47) Hsu, G.; Kalvinskas, J. J. Coal Desulfurization. Chemical and Physical Methods. *ACS Symposium Series*; Wheelock, T. D., Ed.; ACS, 1977.

(48) Ishihara, A.; Nishigori, D.; Saito, M.; Sturisna, I. P.; Qian, W.; Kabe, T. Elucidation of hydrogen mobility in functional groups of coals using tritium tracer methods. *Energy Fuel.* **2002**, *16*, 32−39.

(49) Gao, Y.; Lei, H.; Yin, X.; Zhang, Y.; Huang, Z.; Yin, Y.; Xiao, S.; Wang, P. Study of the Change Laws of Free Radicals and Functional Groups during Coal Oxidation. *ACS Omega* **2023**, *8*, 7102−7110.